ACS Energy LETTERS

http://pubs.acs.org/journal/aelccp

ENERGY FOCUS

Photovoltaics Reaching for the Shockley–Queisser Limit

Cite This: ACS Energy Lett. 2020, 5, 3029–3033

Read Online

ACCESS | Metrics & More | Article Recommendations

Downloaded via AMOLF on September 4, 2020 at 07:52:32 (UTC).
See https://pubs.acs.org/sharingguidelines for options on how to legitimately share published articles.

Since 2016, we have maintained a website[1] that tracks the record efficiency and other performance parameters compared to the thermodynamic Shockley–Queisser (SQ) limit for solar cells made from 14 extensively studied semiconductor materials. In the past four years, solar cells from many of these materials have progressed in efficiency, some very strongly (Figure 1a). This progress is a result of much research effort around the world, recognizing the importance of solar cell efficiency for the future energy supply. Efficiency is a key metric in the development of photovoltaic (PV) systems because the cell cost is only a small fraction of the total cost of a solar power generation system, and hence, increasing efficiency is a near-linear driver for reducing the cost of PV electricity per kilowatt-hour.

Figure 1b compares the key loss factors of each of the materials. We compare the short-circuit current of the record cell (J_{SC}) to the maximum possible short circuit current for that material as calculated from the detailed-balance limit, J_{SQ}. This number $j = J_{SC}/J_{SQ}$ is a measure of photocurrent losses, and a low number indicates that better light management must be applied to improve the solar cell. This includes better incoupling and trapping of light inside the cell and reduction of light absorption in inactive regions of the cell. As a metric for recombination losses, we compare the lowest possible recombination current at the material's bandgap (i.e., the radiative limit), calculated from detailed balance, $J_{0,SQ}$, to the dark recombination current that we derive from the record solar cell data, J_0 (see Methods). A low ratio of $j_0 = J_{0,SQ}/J_0$ indicates that better carrier management by the reduction of bulk and surface recombination is required to improve the solar cell. We plot this metric on a logarithmic scale because the open-circuit voltage (V_{OC}) of a solar cell is logarithmically dependent on the ratio of photocurrent to recombination current.

Much of the focus of the PV research community has recently been on perovskite solar cells, and the resulting progress in their efficiency is stunning. Now the best perovskite cells (efficiency under standard test conditions η = 25.2%) approach the best silicon solar cells (η = 26.7%) in efficiency, despite the far shorter time since their introduction to the research community. As Figure 1b shows, improvements for perovskite cells in the past four years are due to both better carrier and light management. Interestingly, the electrical quality of perovskite cells is now so good that their recombination losses are lower than those of the best silicon solar cells. This is partly explained by the strongly absorbing, direct-bandgap perovskite material, which allows for a much thinner absorber layer compared to what is required with silicon cells. Perovskite solar panels are now being commercialized at several locations in the world. The record efficiency for large (>100 cm^2) perovskite solar cells and panels is still far below that of Si solar panels, and extensive materials processing development will be required to bring these numbers closer. Interestingly, in Si cell technology, records are now often broken in industrial environments, where large-scale manufacturing enables fine-tuning of processing parameters using a large number of cells (though the monocrystalline Si cell record is for a 79 cm^2 area cell).

The 1.1% absolute increase in efficiency for Si cells in the past four years was evenly split between better light management and lower fill factor losses (arising both from reduced series resistance and lower recombination at maximum power point), enabled by an improved heterojunction.[2] The continued dominance of Si on the market means that the impact of new cell designs will be huge if these efficiency improvements are translated to commercial technology. In the last four years, there has already been a massive shift away from the previously dominant Al back surface field (BSF) doping technology (was 80% of the market in 2016[3]) to high-efficiency designs with passivated emitter and contacts (now 70% of the market, mostly passivated emitter and rear contact, PERC[4]). The highest efficiency (>25%) cell technologies using fully passivated contacts ("TOPCON"), interdigitated back contacts (IBC), and heterojunction (HIT) designs[5] are also being developed on an industrial scale and may well become the dominant technology in the coming decade.[4] Further recombination reduction may come from improvements in the Si wafer quality, such as the ongoing shift from p-type Si to n-type Si that is more resistant to transition metal defects, or a change of doping of p-type Si from boron to gallium, to remove boron–oxygen defects.[6] All these developments may enable commercial solar panels with efficiency above 25%. Ultimately, because of the low radiative rate, the efficiency for Si solar cells is limited to 29.4% because of Auger

Received: August 18, 2020
Accepted: August 21, 2020

© XXXX American Chemical Society

https://dx.doi.org/10.1021/acsenergylett.0c01790
ACS Energy Lett. 2020, 5, 3029–3033

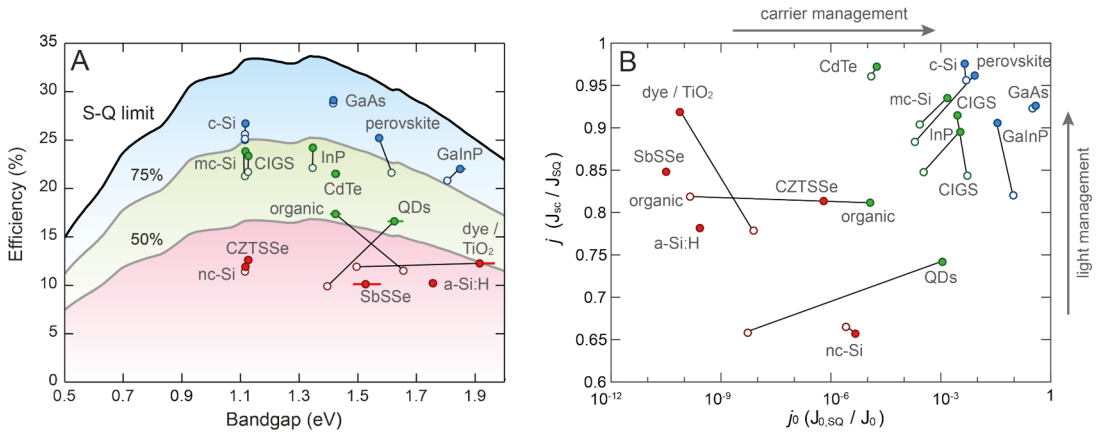

Figure 1. (A) Record efficiency of solar cells of different materials against their bandgap, in comparison to the SQ limit (top solid line). (B) Current density relative to the maximum possible current density, under standardized AM1.5 illumination conditions, versus minimum dark recombination current density relative to the recombination current derived for the record cells in panel A. The open symbols show the record efficiency in April 2016, the solid symbols show the numbers in July 2020.

recombination, 4% below the SQ limit.[7] In principle, this Auger limit could be exceeded by increasing the radiative recombination rate of silicon; a 10-fold increase would already enhance the V_{OC} limit by 60 mV, bringing the efficiency limit up to 31.6%.

Aside from the significant developments in perovskite and silicon solar cells, several other material systems have seen even larger rises in their efficiency. Organic solar cells have benefitted from a range of new molecules that replace the commonly used fullerene acceptor material, like rylene diimide-derivatives and molecules consisting of fused aromatic cores with strong electron-accepting end groups.[8,9] These non-fullerene acceptor cells now reach efficiencies exceeding 17%, mainly enabled by much-reduced recombination losses (Figure 1b). The new acceptor molecules provide a larger tunability of the electron acceptor level, to the extent where the energy loss for exciton dissociation is almost eliminated. Organic solar cells still lose a significant fraction of the photocurrent (around 20%) because of incomplete absorption. Materials with higher charge mobility could enable thicker layers, or nanophotonic structures could increase the light absorption in the thin films. The much lower effective bandgap (1.4 vs 1.6 eV) in the new organic materials also creates potential for higher achievable efficiency (Figure 1a), while the wide-bandgap material combinations are suitable for indoor applications.[10]

The record efficiency of perovskite quantum dot solar cells is 16.6%, which is now far beyond that of the more conventional chalcogenide quantum dot solar cells. They are made from $Cs_{0.5}FA_{0.5}PbI_3$ nanocrystals with a bandgap of 1.6 eV,[11] well above the SQ optimum, suggesting further room for improvement with smaller bandgaps. The perovskite quantum dot record was enabled by reducing both current and recombination losses that are much lower than in the PbS quantum dots that held the record before (Figure 1b). Interestingly, the development of dye-sensitized solar cells has not seen much progress, but historically this research field has served as a fruitful nucleation site for PV materials research of several different kinds, and the narrow absorption spectrum and linear response at different intensities may make them interesting for indoor light-harvesting applications.[12] CdTe cells have shown some progress in efficiency in the past few years (now η = 22.1%) and are a commercial technology. Interestingly, a new earth-abundant material, SbSSe (η = 10.1%), has recently entered the chart.[13]

The overall record for single-junction cells, held by GaAs (η = 29.1%), has seen a small increase in the past four years. Also, many improvements were made in the development of industrial processes, such as the optimization of high-speed chemical vapor deposition processing to industrial manufacturing scale. While relatively expensive at the moment, there are many niche markets with large economic value that can benefit from high-efficiency, flexible, lightweight GaAs cells, such as space and potentially electric vehicle technology. Large-scale introduction in these markets will further drive down the cost of GaAs cell technology, which is also relevant for multi-junction cells, as discussed below.

It is interesting to note that progress is very strong for many different solar cell materials at the moment. The once-separate fields of organic, dye-sensitized, silicon, and quantum dot solar cell research have strongly benefited from shared knowledge and expertise, which yielded synergies, for example in the use of transport layers, processing expertise, and fundamental understanding of materials properties. For example, the development of Si heterojunction cells (composed of crystalline/amorphous heterojunctions) is built on the development of thin-film amorphous Si cells over several decades as well as heterojunction concepts in several other PV materials. Similarly, concepts of selective contact layers and passivation layers are now being shared in many different types of cell materials and designs.

This increased interaction between scientists from different fields is also due to the rise of tandem solar cells as a major research theme, aiming to achieve efficiencies well above 30%. In the past, tandem solar cells were almost exclusively made from combinations of III−V semiconductors, or III−V materials with a silicon base cell. Now, perovskite solar cells are combined with silicon in a 2-terminal or 4-terminal configuration, and perovskite−perovskite and perovskite−copper−indium−gallium−sulfide/selenide (CIGS) tandem cells from different bandgaps allow for high-efficiency thin-film flexible tandem solar cells that can potentially be made at low cost using roll-to-roll processes. The most efficient monolithic two-terminal III−V/Si tandem cell is a triple-junction GaInP/GaAs/Si cell with 33.3% efficiency.[14] For simplicity, we consider only monolithic dual-junction tandem

https://dx.doi.org/10.1021/acsenergylett.0c01790
ACS Energy Lett. 2020, 5, 3029−3033

cells in the following, and the record efficiencies of the five tandem geometries mentioned above are summarized in Table 1. Organic tandem solar cells are also improving with the latest

Table 1. Reported Record Efficiency of Two-Terminal Dual-Junction Solar Cells under AM1.5 Illumination, Bandgaps of the Subcells, Tandem SQ Limit-Efficiency for these Bandgaps, and Calculated Tandem Efficiency Based on Subcell Losses in Figure 1b

tandem materials combination	record efficiency (%)	bandgaps (eV)	SQ limiting efficiency (%)	SQ efficiency with losses (%)
GaInP/GaAs	32.8	1.95/1.42	40.4	34.8
perovskite/Si	29.2	1.70/1.12	44.1	35.7
perovskite/perovskite	24.2	1.82/1.27	40.9	33.2
perovskite/CIGS	24.2	1.70/1.13	43.6	32.8
GaAsP/Si	23.4	1.73/1.12	44.9	

record organic material combinations, even though the current record organic tandem solar cell is still less efficient than the best single-junction cell, and is left out of the further analysis here.

The GaInP/GaAs tandem cell (η = 32.8%) shows an efficiency well above that of the record for the individual cells (η = 22.0%/29.1%). A major breakthrough is the fact that perovskite/Si tandems have just recently significantly exceeded the record for the Si-only cell (η = 29.2% versus 26.7%). Perovskite−perovskite and perovskite−CIGS tandems have efficiencies close to the single-junction values, and further materials and device improvements are needed to exceed these. The maximum achievable efficiency according to the SQ model, using the indicated bandgaps as input, is also shown in Table 1. We can predict a more realistic multijunction cell efficiency limit taking into account the photocurrent and recombination losses in the individual subcells, as in Figure 1a. As a first-order estimate, we take the values for $J_{SC}/J_{SC,SQ}$, $V_{OC}/V_{OC,SQ}$ from Figure 1b and the fill factor relative to the SQ value (FF/FF_{SQ}) for the individual materials and use these as input to calculate a single-junction-derived maximum efficiency of the corresponding multijunction geometry (see Table 1). All the tandem cell records are well below these more realistic numbers, indicating much room for improvement in the tandem geometries themselves, taking into account the subcell records achieved to date. Further improvements will be achievable as the subcell efficiencies improve further.

In practice, fabrication, materials, and cell design constraints cause the achievable multijunction cell efficiency to be well below the limiting values calculated based on losses for individual cells (compare gray points in Figure 2 to colored points). We list a few examples. In many multijunction cells, incomplete current matching between the subcells and/or incomplete light absorption in the top cell reduces the efficiency. The record III−V/Si tandems are made using wafer-bonding, requiring the top-surface of the Si bottom cell to be flat, which reduces light trapping in the Si cell that is usually achieved by texturing the surface. For the 2-junction GaAsP/Si cell this loss results in a photocurrent loss of 19% compared to the detailed-balance limit (Figure 2). The lattice mismatch also introduces dislocations, reducing the $v \times f$. In addition, the very high efficiency in the record single-junction GaAs cells is achieved by photon recycling using a low-loss

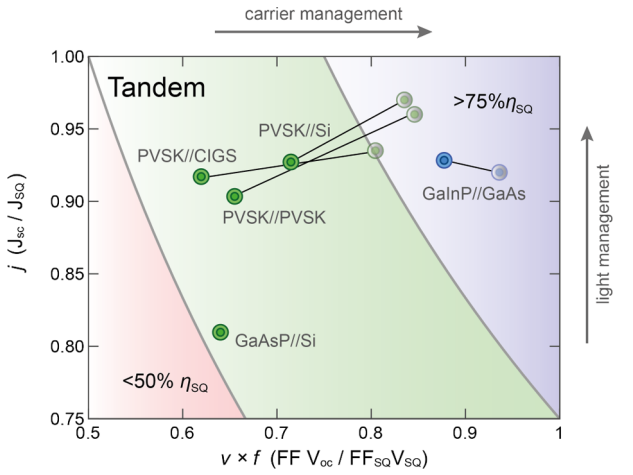

Figure 2. Current density of selected tandem cells relative to the maximum possible current density, under standardized AM1.5 illumination conditions, versus open-circuit voltage−fill factor product relative to the maximum possible values according to the SQ model. The filled symbols show the experimental data. The gray symbols show calculated data for tandem cells based on numbers for the single-junction record cells.

back reflector[15] which cannot be fully translated to a tandem geometry.

Perovskite/silicon tandem cells, where a textured silicon base cell can be used when the perovskite cell is processed from the vapor phase, show a photocurrent much closer to the limit with only 7% loss. For all tandem cells with a perovskite top cell the low dark recombination current found for the record single-junction cell has not been achieved in perovskite cells with the higher and lower bandgaps that are required for the tandem geometry. This difference can be seen from the difference of the gray points (single-junction derived efficiency limit) to the green points in Figure 2. For the highest bandgap perovskites (pure bromide), the V_{OC} loss comes primarily from interfacial recombination, particularly at the electron-selective contact.[16] In state-of-the-art mixed halide systems, the loss is roughly split evenly between nonradiative recombination at bulk and interfacial (contact) traps, with halide segregation playing a minor role.[17,18] For the lowest bandgap materials (Pb−Sn perovskites), there has not been a thorough study of the remaining V_{OC} losses. The optoelectronic quality is already at the same level as the pure lead iodide perovskites, suggesting that interfacial recombination may be the biggest remaining loss mechanism.[19] Additionally, in general, selective contacts and buffer and passivation layers used for record single-junction cells are not always compatible with the multijunction design.

While the studies toward record efficiency continuously inspire novel developments in PV materials, the choice of the most suitable PV material will be influenced by its practical application. Solar panels placed in hot regions on earth are best made of materials that have a very low temperature coefficient of efficiency. Large-scale implementation of PV in solar fields will require bifacial solar panels[20] that are optimized for the highest power harvesting integrated over the day. For integration of PV in building materials, proven long-term stability is a key parameter. For all materials, circular materials processing and low use of scarce and toxic materials are critical for large-scale implementation.

https://dx.doi.org/10.1021/acsenergylett.0c01790
ACS Energy Lett. 2020, 5, 3029−3033

Ultimately, the record efficiency in the lab needs to be translated into a high module efficiency to be of commercial relevance. Here the established technologies have a clear advantage. The best Si and CdTe modules perform only 3% (abs.) below the lab record efficiency, while that difference is about 4% (abs.) for GaAs. For perovskite and organic solar cells that difference is larger. The best organic modules are currently below 12% efficiency, almost 6% (abs.) below their lab cell record, and perovskite modules at 18% are performing 7% (abs.) worse than the lab record. Also, the record modules fabricated from the emerging technologies are smaller (organic, 204 cm^2; perovskite, 802 cm^2) than the modules made from established technologies (e.g., Si with 13 177 cm^2).[21] Clearly, much is to be gained from progress in processing, scaling up, and module fabrication.

The field of solar cell materials development is at an exciting, dynamic stage. Silicon PV dominates the market, and cell and module efficiencies continue to improve. New materials enable multijunction solar cells (based on Si or other materials combinations) with further improved efficiency that may find their way to very large-scale power generation in solar fields. Other materials with new functionality, such as low weight, mechanical flexibility, and colored appearance, enable a wide range of new applications in building- and landscape-integrated PV.

METHODS

Calculation of $J_{0,SQ}$ and $J_{0,exp}$. The limiting values for $J_{0,SQ}$ according to the SQ model were calculated using the Shockley diode equation for a solar cell under illumination, assuming an ideal diode:

$$J = J_{SC} - J_0\left(\exp\left[\frac{qV}{k_BT}\right] - 1\right)$$

At $V = V_{OC}$, the $J = 0$ and we can write

$$J_0 = J_{SC}\left(\exp\left[\frac{qV_{OC}}{k_BT}\right] - 1\right)^{-1}$$

with the SQ-values for J_{SC} and V_{OC} known for each bandgap, with which the corresponding SQ–J_0 values can be obtained. The experimental $J_{0,exp}$ value for each solar cell was obtained in the same way, using the corresponding experimental V_{OC} and J_{SC} values under standard test conditions (AM1.5G spectrum, 1000 W/m^2, 25 °C). Note that this is a first-order analysis that does not take into account many factors, including series and shunt losses.

The bandgap was determined using the external quantum efficiency (EQE) curves for the record cells. The low-energy tail of the EQE was fitted on a log-scale as a function of energy. Linear functions were fitted to the tail, with a variation of different limits for the data range. The fitted line that minimized the residuals was chosen as best fit. The energy value for which this fitted line reaches the max-EQE value yields the bandgap. Quite consistently, the value where the EQE reaches approximately 50% corresponds to this bandgap. We note that the absolute value of the bandgap depends on the choice of fitting method,[22] but that the comparison between materials (and hence bandgaps) with the same fitting method yields very similar relative differences.

Calculation of 2T-Tandem SQ Efficiencies. The 2T-tandem SQ limits are calculated based on an extension of the single-junction detailed-balance calculation.[23] For each subcell, J_{SC}, V_{OC}, and *IV*-curves (for FF) are computed. The tandem-J_{SC} is obtained by using the current-matching condition, taking the smallest subcell J_{SC} as tandem-J_{SC}. The tandem-V_{OC} is taken as the sum of the subcells' V_{OC} values. The tandem *IV*-curve (which then yields the tandem-FF) is calculated by applying the current-matching condition to every point across the *IV*-curves of the two subcells. Starting at $J = 0$, for each J value up to $J_{SC,tandem}$, corresponding voltage pairs of the subcells' *IV*-curves can be found, and their sum gives the tandem's *V*-value for that specific current J. From these SQ-tandem values, together with the experimental values from ref 24, the SQ-fractions are obtained. A similar analysis was performed to calculate the tandem efficiencies based on the values of individual record subcells.

Bruno Ehrler orcid.org/0000-0002-5307-3241
Esther Alarcón-Lladó orcid.org/0000-0001-7317-9863
Stefan W. Tabernig
Tom Veeken
Erik C. Garnett orcid.org/0000-0002-9158-8326
Albert Polman orcid.org/0000-0002-0685-3886

AUTHOR INFORMATION

Complete contact information is available at:
https://pubs.acs.org/10.1021/acsenergylett.0c01790

Notes

Views expressed in this Energy Focus are those of the authors and not necessarily the views of the ACS.
The authors declare no competing financial interest.

ACKNOWLEDGMENTS

This work is part of the research program of the Dutch Research Council (NWO).

REFERENCES

(1) AMOLF SQ Charts. https://www.lmpv.nl/sq/ (accessed 2020-08-03).
(2) Yoshikawa, K.; Kawasaki, H.; Yoshida, W.; Irie, T.; Konishi, K.; Nakano, K.; Uto, T.; Adachi, D.; Kanematsu, M.; Uzu, H.; Yamamoto, K. Silicon Heterojunction Solar Cell with Interdigitated Back Contacts for a Photoconversion Efficiency over 26%. *Nat. Energy* **2017**, *2*, 17032.
(3) Metz, A.; Fischer, M.; Trube, J. *International Technology Roadmap for Photovoltaics (ITRPV)*, 8th ed.; Itrpv, 2017.
(4) ITRPV. *International Technology Roadmap for Photovoltaic*, 11th ed; 2019.
(5) Polman, A.; Knight, M.; Garnett, E. C.; Ehrler, B.; Sinke, W. C. Photovoltaic Materials – Present Efficiencies and Future Challenges. *Science (Washington, DC, U. S.)* **2016**, *352*, aad4424.
(6) Geerligs, L. J.; G, N.; R, I. G. Progression of N-Type Base Crystalline Silicon Solar Cells. *Photovoltaics Int.* **2011**, *12*, 94–102.
(7) Richter, A.; Hermle, M.; Glunz, S. W. Reassessment of the Limiting Efficiency for Crystalline Silicon Solar Cells. *IEEE J. Photovoltaics* **2013**, *3*, 1184–1191.
(8) Yan, C.; Barlow, S.; Wang, Z.; Yan, H.; Jen, A. K. Y.; Marder, S. R.; Zhan, X. Non-Fullerene Acceptors for Organic Solar Cells. *Nat. Rev. Mater.* **2018**, *3*, 18003.
(9) Hou, J.; Inganas, O.; Friend, R. H.; Gao, F. Organic Solar Cells Based on Non-Fullerene Acceptors. *Nat. Mater.* **2018**, *17*, 119–128.
(10) Cui, Y.; Wang, Y.; Bergqvist, J.; Yao, H.; Xu, Y.; Gao, B.; Yang, C.; Zhang, S.; Inganäs, O.; Gao, F.; Hou, J. Wide-Gap Non-Fullerene Acceptor Enabling High-Performance Organic Photovoltaic Cells for Indoor Applications. *Nat. Energy* **2019**, *4*, 768–775.

(11) Hao, M.; Bai, Y.; Zeiske, S.; Ren, L.; Liu, J.; Yuan, Y.; Zarrabi, N.; Cheng, N.; Ghasemi, M.; Chen, P.; Lyu, M.; He, D.; Yun, J. H.; Du, Y.; et al. Ligand-Assisted Cation-Exchange Engineering for High-Efficiency Colloidal Cs1−xFAxPbI3 Quantum Dot Solar Cells with Reduced Phase Segregation. *Nat. Energy* **2020**, *5*, 79−88.
(12) Freitag, M.; Teuscher, J.; Saygili, Y.; Zhang, X.; Giordano, F.; Liska, P.; Hua, J.; Zakeeruddin, S. M.; Moser, J.-E.; Grätzel, M.; Hagfeldt, A. Dye-Sensitized Solar Cells for Efficient Power Generation under Ambient Lighting. *Nat. Photonics* **2017**, *11*, 372−378.
(13) Tang, R.; Wang, X.; Lian, W.; Huang, J.; Wei, Q.; Huang, M.; Yin, Y.; Jiang, C.; Yang, S.; Xing, G.; Chen, S.; Zhu, C.; Hao, X.; Green, M. A.; et al. Hydrothermal Deposition of Antimony Selenosulfide Thin Films Enables Solar Cells with 10% Efficiency. *Nat. Energy* **2020**, *5*, 587−595.
(14) Cariou, R.; Benick, J.; Feldmann, F.; Höhn, O.; Hauser, H.; Beutel, P.; Razek, N.; Wimplinger, M.; Bläsi, B.; Lackner, D.; Hermle, M.; Siefer, G.; Glunz, S. W.; Bett, A. W.; et al. III-V-on-Silicon Solar Cells Reaching 33% Photoconversion Efficiency in Two-Terminal Configuration. *Nat. Energy* **2018**, *3*, 326−333.
(15) Walker, A. W.; Höhn, O.; Micha, D. N.; Bläsi, B.; Bett, A. W.; Dimroth, F. Impact of Photon Recycling on GaAs Solar Cell Designs. *IEEE J. Photovoltaics* **2015**, *5*, 1636−1645.
(16) Zohar, A.; Kulbak, M.; Levine, I.; Hodes, G.; Kahn, A.; Cahen, D. What Limits the Open-Circuit Voltage of Bromide Perovskite-Based Solar Cells? *ACS Energy Lett.* **2019**, *4*, 1−7.
(17) Mahesh, S.; Ball, J. M.; Oliver, R. D. J.; McMeekin, D. P.; Nayak, P. K.; Johnston, M. B.; Snaith, H. J. Revealing the Origin of Voltage Loss in Mixed-Halide Perovskite Solar Cells. *Energy Environ. Sci.* **2020**, *13*, 258−267.
(18) Guo, Z.; Jena, A. K.; Takei, I.; Kim, G. M.; Kamarudin, M. A.; Sanehira, Y.; Ishii, A.; Numata, Y.; Hayase, S.; Miyasaka, T. V OC Over 1.4 V for Amorphous Tin-Oxide-Based Dopant-Free CsPbI 2 Br Perovskite Solar Cells. *J. Am. Chem. Soc.* **2020**, *142*, 9725−9734.
(19) Klug, M. T.; Milot, R. L.; Patel, J. B.; Green, T.; Sansom, H. C.; Farrar, M. D.; Ramadan, A. J.; Martani, S.; Wang, Z.; Wenger, B.; Ball, J. M.; Langshaw, L.; Petrozza, A.; Johnston, M. B.; et al. Metal Composition Influences Optoelectronic Quality in Mixed-Metal Lead−Tin Triiodide Perovskite Solar Absorbers. *Energy Environ. Sci.* **2020**, *13*, 1776−1787.
(20) Coletti, G.; Luxembourg, S. L.; Geerligs, L. J.; Rosca, V.; Burgers, A. R.; Wu, Y.; Okel, L.; Kloos, M.; Danzl, F. J. K.; Najafi, M.; Zhang, D.; Dogan, I.; Zardetto, V.; Di Giacomo, F.; et al. Bifacial Four-Terminal Perovskite/Silicon Tandem Solar Cells and Modules. *ACS Energy Lett.* **2020**, *5*, 1676−1680.
(21) NREL. Champion Photovoltaic Module Efficiency Chart, https://www.nrel.gov/pv/module-efficiency.html (accessed 2020-08-21).
(22) Krückemeier, L.; Rau, U.; Stolterfoht, M.; Kirchartz, T. How to Report Record Open-Circuit Voltages in Lead-Halide Perovskite Solar Cells. *Adv. Energy Mater.* **2020**, *10*, 1902573.
(23) Futscher, M. H.; Ehrler, B. Efficiency Limit of Perovskite/Si Tandem Solar Cells. *ACS Energy Lett.* **2016**, *1*, 863−868.
(24) Green, M. A.; Dunlop, E. D.; Hohl-Ebinger, J.; Yoshita, M.; Kopidakis, N.; Hao, X. Solar Cell Efficiency Tables (Version 56). *Prog. Photovoltaics* **2020**, *28*, 629−638.

https://dx.doi.org/10.1021/acsenergylett.0c01790
ACS Energy Lett. 2020, 5, 3029−3033